Available online at www.sciencedirect.com

ScienceDirect

Procedia Materials Science 3 (2014) 21 – 26

Procedia Materials Science

www.elsevier.com/locate/procedia

20th European Conference on Fracture (ECF20)

Micromechanical modeling of creep damage in a Copper-Antimony Alloy

Markus Vöse[a], Bernard Fedelich[a]*, Frederik Otto[b], Gunther Eggeler[b]

[a]*Federal Institute for Materials Research and Testing (BAM), Berlin, Germany*
[b]*Ruhr-University Bochum, Bochum, Germany*

Abstract

A micromechanical model of creep induced grain boundary damage is proposed, which allows for the simulation of creep damage in a polycrystal with the finite element method. Grain boundary cavitation and sliding are considered via a micromechanically motivated cohesive zone model, while the grains creep following the slip system theory. The model has been calibrated with creep test data from pure Cu single crystals and a coarse-grained polycrystalline Cu-Sb alloy. The test data includes porosity measurements and estimates of grain boundary sliding. Finally, the model has been applied to Voronoi models of polycrystalline structures. In particular the influence of grain boundary sliding on the overall creep rate is demonstrated.

Selection and peer-review under responsibility of the Norwegian University of Science and Technology (NTNU), Department of Structural Engineering

Keywords: Creep damage; grain boundary sliding; cohesive zone; micromechanical model; polycrystal.

1. Introduction

In many practical applications, creep damage is the limiting factor of a component's lifetime. In an ongoing research, a model has been developed to bridge the scales of the individual creep cavities and of the polycrystal. The link between these scales is a cohesive zone model that accounts for the effective mechanical behavior of the Grain Boundaries (GB) subjected to normal and tangential stresses. It accounts for GB thickening as well as GB sliding.

* Corresponding author. Tel.: +49 30 8104 3104; fax: +49 30 8104 1527.
E-mail address: bernard.fedelich@bam.de

Selection and peer-review under responsibility of the Norwegian University of Science and Technology (NTNU), Department of Structural Engineering
doi:10.1016/j.mspro.2014.06.006

The development of the model has been previously presented (Fedelich and Owen, 2009; Vöse et al., 2012; Vöse et al., 2014). The present paper summarizes the model equations and its calibration and introduces first applications to Representative Volume Elements (RVE) of polycrystals.

2. A cohesive zone model for grain boundary creep damage

2.1. Model summary

For an exposition of the theory of GB cavitation under creep loading in metals, the reader may refer to the seminal textbook of Riedel (1987). In the following, the local state of damage on a GB is represented by two variables:

- The surface cavity density $\rho = N_S / S_0$, where N_S is the number of cavities in an element S_0 of the GB surface
- The dimensionless damage variable $\beta = V_S / S_0 \sqrt{\rho}$, where V_S is the cumulated volume of the cavities contained in S_0

Note that the quantity defined by $u_n^{\,p} = V_S / S_0$ corresponds to the average thickening of the GB. Accordingly, β can also be written as $\beta = u_n^{\,p} \sqrt{\rho}$ and thus regarded as the GB thickening scaled by the average cavity spacing. Evolutions equations for these variables

$$\begin{aligned} \dot{\rho} &= \dot{\rho}\left(\rho, \beta; a_{\text{init}}, \tilde{D}_{gb}, \gamma_s, a_p, b_p, \psi\right), \\ \dot{\beta} &= \dot{\beta}\left(\rho, \beta; a_{\text{init}}, \tilde{D}_{gb}, \gamma_s, a_p, b_p, \psi\right), \end{aligned} \tag{1}$$

have been derived by Vöse et al. (2012), and modified and presented in their final form in Vöse et al. (2014). They rely on the detailed simulations of cavitation in an element of GB following the procedure developed by Fedelich and Owen (2009) and Vöse et al. (2012). Cavity growth by GB diffusion and cavity coalescence are considered herein. Cavity nucleation is random and stress driven according to the power law

$$\dot{\rho}^{nucleation} = a_p \left(\frac{\sigma_n}{\sigma_p} \right)^{b_p} \tag{2}$$

for the nucleation rate, where σ_n is the normal stress acting on the GB, σ_p is a reference stress and a_p and b_p are two adjustable model parameters. The remaining parameters in equ. (1) are a_{init} the initial radius of new cavities, ψ the dihedral angle, γ_s the specific energy per unit area and $\tilde{D}_{gb}$ the GB diffusion coefficient. To bridge the cavity scale and the polycrystal scale, the contributions of the individual cavities to GB thickening and stiffness decrease are smeared over the GB, as proposed by Onck and Van der Giessen (1997). The net effect of cavitation at the polycrystal level is represented by the displacement jump

$$\mathbf{u} = \mathbf{u}^{\text{grain 1}} - \mathbf{u}^{\text{grain 2}} = u_n \, \mathbf{n} + u_t \, \mathbf{t}, \tag{3}$$

where $\mathbf{u}^{\text{grain 1}}$ and $\mathbf{u}^{\text{grain 2}}$ are the displacements of material points attached to the adjoining grains along the GB (see Fig. 1) and $\mathbf{n}$ resp. $\mathbf{t}$ is the normal resp. a tangential vector to the GB.

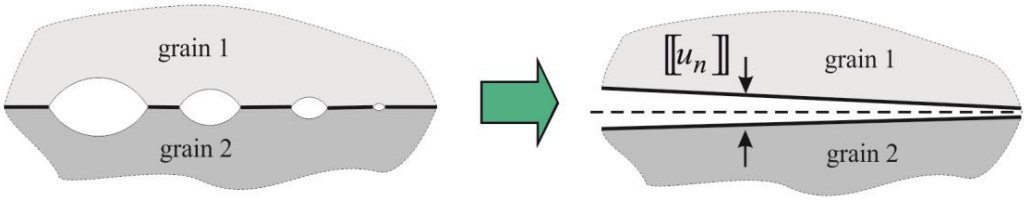

Fig. 1. smearing the contributions of individual cavities to GB thickening.

The displacement jump also admits the decomposition

$$\mathbf{u} = \mathbf{u}^{el} + \mathbf{u}^{inel}, \tag{4}$$

in an elastic $\mathbf{u}^{el}$ and an inelastic contribution $\mathbf{u}^{inel}$. The elastic part $\mathbf{u}^{el}$ is introduced as a way to account for the loss of stiffness of the polycrystal consecutive to cavitation. It is related to the stress vector on the GB $\boldsymbol{\sigma}\cdot\mathbf{n}$ by a linear relationship

$$\boldsymbol{\sigma}\cdot\mathbf{n} = \mathbf{D}(\beta,\rho)\cdot\mathbf{u}^{el}. \tag{5}$$

The matrix $\mathbf{D}(\beta,\rho)$ represents the reduction of the effective stiffness of the GB as function of the damage state. It has been identified by Vöse (2010) by estimating the loss of stiffness of bicrystal models with a GB weakened by cavities. The normal component u_n^{inel} of the inelastic part is directly related to GB thickening via

$$u_n^{inel} = \frac{\beta}{\sqrt{\rho}} - \frac{\beta_0}{\sqrt{\rho_0}}, \tag{6}$$

where ρ_0 and β_0 are the initial values of the damage variables. The tangential component $u_t^{inel} \equiv u_t^{slide}$ of the inelastic jump along $\mathbf{t} = \overrightarrow{\boldsymbol{\sigma}\cdot\mathbf{n} - (\mathbf{n}\cdot\boldsymbol{\sigma}\cdot\mathbf{n})\mathbf{n}}$ reflects GB sliding. It is assumed to follow the linear viscous law

$$\dot{u}_t^{slide} = \frac{\tau}{\eta_{slide}}, \tag{7}$$

where η_{slide} is a viscosity coefficient and $\tau = \left\|\boldsymbol{\sigma}\cdot\mathbf{n} - (\mathbf{n}\cdot\boldsymbol{\sigma}\cdot\mathbf{n})\mathbf{n}\right\|$ the shear stress component in the GB. Finally, the mechanical behaviour of the grains has been modelled by single crystal viscoplasticity. The constitutive law at hand accounts for isotropic hardening and has a power law for the shear rates at the slip system level.

2.2. Model identification

The cohesive zone model presented in section 2.1 contains the material dependent parameters a_{init}, $\tilde{D}_{gb}$, γ_s, a_p, b_p, ψ, and η_{slide}, but the available experimental data didn't allow for an unambiguous determination of all parameters. The simulations performed by Vöse et al. (2012) revealed that the parameters $\tilde{D}_{gb}$, a_p and b_p have the highest influence on the cavitation process. Hence these parameters have been identified by using exp. data as

explained below. The remaining values have been taken from the literature or set to plausible values. The dihedral angle has been set to $\psi = 70°$, the initial radius for newly nucleated cavities to $a_{\text{init}} = 1\mu\text{m}$ and for the specific energy of a free surface the value $\gamma_s = 1.78\,\text{Jm}^{-2}$ after Wang et al. (1983) has been adopted. The reference stress in equ. (2) has been taken as the shear modulus of copper $\sigma_p = 42\,\text{GPa}$. The remaining parameters have been estimated by solving an inverse problem. For the creep simulations, the GB and grain material models have been implemented as UMAT user subroutines of the ABAQUS software (http://www.3ds.com/products-services/simulia/). Note that GB cavitation is simulated until a damaged area fraction $\omega = 0.5$ is reached. Beyond this value, the stiffness of the cohesive zone elements is set to zero. The estimation procedure has consisted in the following steps:

- First the parameters of the crystal viscoplastic model for the grains have been identified. For this purpose creep tests with miniature tensile creep specimens (see, e.g., Mälzer 2007) of pure Cu single crystals have been performed at 823 K.
- Creep tests with miniature specimens of a coarse-grained polycrystalline Cu-Sb alloy (grain size around 1mm) have been performed at 823 K (see Fig 2a). The grain structure of the specimens has been characterized by the EBSD method and GB sliding by Digital Image Correlation (DIC). The tests have been simulated by FE (see Fig. 2b) and a magnitude $\eta_{\text{slide}} = 4\times10^{7}\,\text{Ns/mm}^3$ of the viscosity coefficient was found to best reproduce the DIC results.
- The parameters $\tilde{D}_{gb}$, a_p and b_p have been adjusted to reproduce the damage measurements on polished sections of the coarse-grained specimens. Since the number of cavities per GB in a section was too low to enable an evaluation of the damage variables (ρ,β) at the GB level, the total cavities number and the cumulated apparent cavities surface in specimens polished sections have been used for comparison.

Fig. 2. (a) miniature creep specimens; (b) 3D FE model of the grain structure in the gauge length.

In view of the lack of data for a sufficiently large range of stresses it was not possible to uniquely estimate the stress exponent b_p of equ. (2). However, large values of b_p could be ruled out by qualitative comparisons of the damage distribution on the GBs between the tested and the simulated specimens. Indeed the simulations have demonstrated that stress concentrations occur at triple junctions due to GB sliding. Hence, a high stress exponent promotes wedge-type damage at GB triple junctions. It was found that the value $b_p = 5$ yielded a clear overestimation of the number of wedge cracks at triple junctions. Thus a low exponent $b_p = 1$ has been retained and the remaining parameters $\tilde{D}_{gb} = 10^{-14}\,\text{mm}^5\text{N}^{-1}\text{s}^{-1}$ and $a_p = 2\times10^{2}\,\text{mm}^{-2}\text{s}^{-1}$ have been adjusted to the test data.

3. Application to a Representative Volume Element of a polycrystal

This section presents the first applications to RVEs of a polycrystal. The grain structure is based on a periodic 3D Voronoi tessellation (see, e.g., Fritzen et al., 2009). The grains have been meshed with linear tetrahedral elements using the NETGEN library (http://sourceforge.net/projects/netgen-mesher/). An example of a RVE is shown in Fig. 3a and the damaged GBs after 40 h creep under 10 MPa are displayed in Fig. 3b.

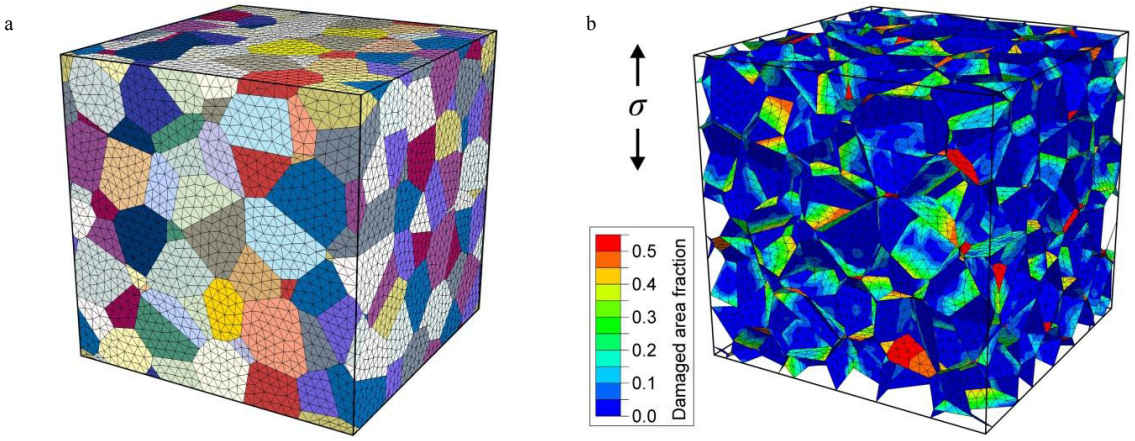

Fig. 3. (a) FE model of a RVE with 216 grains; (b) cavitated area fraction of the GBs.

Creep tests with a finer grained alloy (average grain size around 0.3 mm) have been performed by Otto et al. (2012) and simulated. Fig. 4a shows that a number of 216 grains is sufficient to obtain a representative creep curve. However, a significant influence of mesh refinement can be observed for the 16 grains RVE (degrees of freedom: coarse – 12696, medium – 26229, fine – 313281), in which the fine mesh yields the highest stationary creep rate. In Fig. 4b, the viscosity parameter has been increased resp. decreased by a factor of 1000 with respect to its value identified in the previous section. The high value of η_{slide} roughly corresponds to sliding-free GBs while the low value to almost perfectly sliding GBs. Clearly, GB sliding has a significant contribution to the creep rate, a fact that was already observed in the coarse-grained specimens by Vöse et al. (2014). Note that since the grain structure at hand is fully 3D, constraining of GB sliding by the surrounding grains could be expected, which would reduce the contribution of GB sliding to the creep rate. However, Fig. 4b shows that GB sliding is not noticeably constrained. On the other side, GB sliding seems to have a limited influence on the onset of tertiary creep.

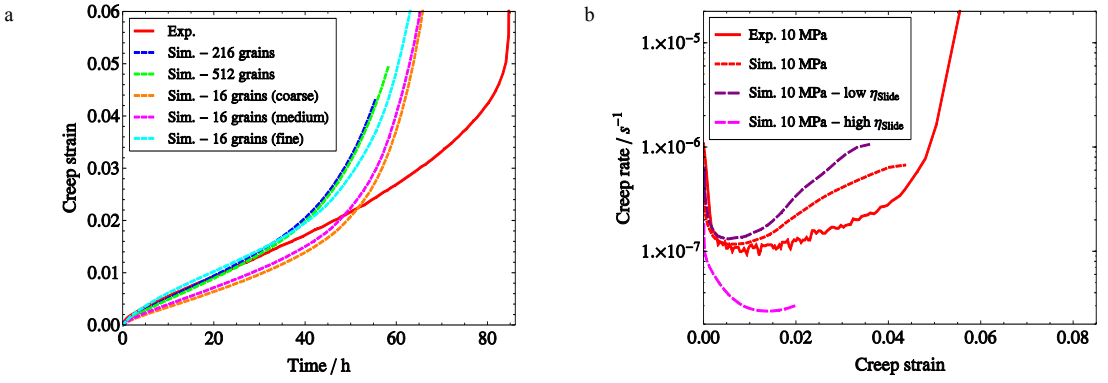

Fig. 4. (a) influence of mesh refinement and number of grains at 10MPa stress level; (b) influence of GB sliding at 10MPa stress level.

The minimum creep rate is well predicted at 10MPa while it is underestimated at higher stresses (see Fig. 5a). Also the amount of primary creep is overestimated at higher stresses. Comparison with Fig. 4a suggests that an influence of meshing cannot be excluded in this respect, a point that needs to be further investigated in the future. Finally, it can be observed that the predicted creep rate acceleration doesn't continuously increase, in contrast to the experimental data. This is likely due to the fact that cavitation is dominated by GB diffusion in the present model. However, for high stresses or high damaged area fractions, the cavities increasingly grow by dislocation creep, a mechanism that can be neglected in the early stages of cavitation. However, an accurate description of the tertiary creep curve is usually not critical for practical purposes. Instead, the prediction of the onset of tertiary creep is essential, which, apart from the highest stress level, is well predicted by the model (see Fig. 5b).

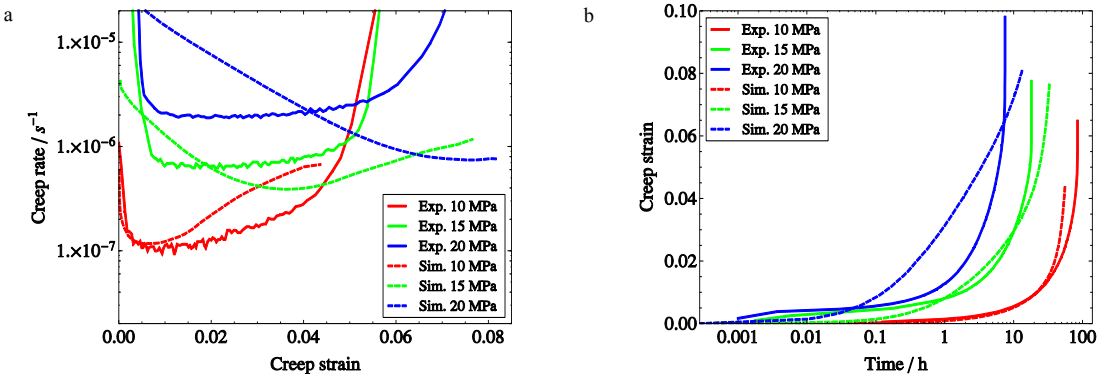

Fig. 5. (a) influence of stress level on the creep rate; (b) influence of stress level on the creep curve.

Acknowledgements

The authors gratefully acknowledge financial support from the German Research Foundation (DFG). They also thank Professor Hartmaier of the RUB for helpful discussions. Finally the authors gratefully acknowledge the work of Dieter Noack and Cetin Haftaoglu who implemented the single crystal creep model as a UMAT subroutine.

References

Fedelich, B., Owen, J., 2009. Creep Damage by Multiple Cavity Growth Controlled by Grain Boundary Diffusion. Proceedings of the 12th International Conference on Fracture, Ottawa, Canada, July 12-17.

Fritzen, F., Böhlke, T., Schnack, E., 2009. Periodic three-dimensional mesh generation for crystalline aggregates based on Voronoi tessellations. Comp. Mech. 43, 701-713.

Mälzer, G., Hayes, R.W., Mack, T., Eggeler, G., 2007. Miniature Specimen Assessment of Creep of the Single-Crystal Superalloy LEK 94 in the 1000°C Temperature Range. Metall. Mat. Trans. 38 A, 314-327.

Onck, P., Van der Giessen, E., 1997. Microstructurally-based modelling of intergranular creep fracture using grain elements. Mech. Mater. 26 109-126.

Otto, F., Viswanathan, G. B., Payton, E. J., Frenzel, J., Eggeler, G., 2012. On the effect of grain boundary segregation on creep and creep rupture. Acta Mat. 60, 2982-2998.

Riedel, H., 1987. Fracture at High Temperatures, Springer Verlag.

Vöse, M., Fedelich, B., Owen, J., 2012. A simplified model for creep induced grain boundary cavitation validated by multiple cavity growth simulations. Comp. Mater. Sci. 58, 201-213.

Vöse, M., 2010. Bestimmung der effektiven Steifigkeit eines an den Korngrenzen geschädigten Polykristalls. TU Berlin, Diploma Thesis.

Vöse, M., Otto, F., Fedelich, B., Eggeler, G., 2014. Micromechanical investigations and modelling of a copper-antimony-alloy under creep conditions. Mechanics of Materials 69, 41-62.